Disappearance of flow as a probe of the nuclear equation of state

D. Krofcheck,* W. Bauer, G. M. Crawley, S. Howden, C. A. Ogilvie,†
A. Vander Molen, G. D. Westfall, and W. K. Wilson‡
National Superconducting Cyclotron Laboratory and Department of Physics and Astronomy, Michigan State University, East Lansing, Michigan 48824

R. S. Tickle
Department of Physics, University of Michigan, Ann Arbor, Michigan 48109

C. Djalali
Department of Physics, University of South Carolina, Columbia, South Carolina 29208

C. Gale
Department of Physics, McGill University, Montreal, Quebec, Canada H3A 2T8
(Received 13 February 1992)

The disappearance of directed, collective nuclear motion ("flow") away from the interaction region of heavy-ion collisions has been observed using the Lawrence Berkeley Laboratory Streamer Chamber. We find that flow vanishes at a beam energy near 50 MeV/nucleon for the ^{139}La+^{139}La system and near 60 MeV/nucleon for the ^{93}Nb+^{93}Nb system. The disappearance of flow may be understood as resulting from a balance between attractive and repulsive scattering strengths. Full calculations with the Boltzmann-Uehling-Uhlenbeck model show that the disappearance of flow is sensitive to the assumed nuclear equation of state (EOS) and to the in-medium scattering cross section (σ_{NN}). Also, in the ^{93}Nb+^{93}Nb system, the purely attractive contribution to the reduced flow does not appear to be strongly sensitive to the EOS assumptions.

PACS number(s): 25.70.Pq

I. INTRODUCTION

One of the most alluring goals of contemporary heavy-ion physics is the complete determination of the nuclear matter equation of state (EOS). The EOS can be expressed as the relationship between the energy needed to compress nuclear matter and the nuclear density. At low densities this relationship is essentially fixed by the properties of ground state nuclear matter. The situation is more ambiguous for higher densities where the EOS has been characterized by a variety of nuclear compressibility (K) values. Theoretical work on Fermi-liquid theory [1] and an analysis of nuclear collective flow that employs Boltzmann-Uehling-Uhlenbeck (BUU) calculations [2] that include a momentum-dependent interaction [3] suggest that K is near 100 or 215 MeV, respectively. Measurements of the position of the giant monopole resonance in Sn and Sm isotopes [4] imply that K is nearer to 300 MeV. An analysis [5] of neutron star mass measurements concludes that $K \geq 225$ MeV is reasonable. Results from a study [6] of pion production from high-energy heavy-ion collisions imply that K may be closer to 375 MeV. It is clear that uncertainties in the theoretical models and in the interpretation of experimental data can lead to a broad range in the deduced value for the compressibility [5].

An alternative experimental approach is to use the vanishing of directed collective motion in intermediate energy heavy-ion collisions, or the disappearance of flow [7, 8], to determine the compressibility. Directed collective motion occurs whenever the measured average in-plane transverse momentum is in opposite directions for nuclear fragments emitted in the forward and backward center-of-mass hemispheres. Variations in such motion as a function of beam energy reflect the competition between attractive and repulsive scattering [9]. The evolution from a predominantly attractive to repulsive reaction mechanism is illustrated at two bombarding energies: at $E/A = 35$ MeV where the attractive mean field was shown [10] to pull fragments to negative scattering angles, and at $E/A = 100$ MeV where increased compressional potential energy and individual N-N scatterings should repel fragments towards positive scattering angles [11]. Flow disappears when the strengths of the two competing reaction mechanisms are balanced.

The disappearance of flow is a robust observable in measurements of collective motion from heavy-ion colli-

*Present address: Lawrence Livermore National Laboratory, Livermore, CA 94550.
†Present address: Gesellschaft für Schwerionenforschung, Darmstadt, Germany.
‡Present address: Lawrence Berkeley Laboratory, Berkeley, CA 94720.

sions. This is because the disappearance is unaffected by the dispersion of the estimated reaction plane about the true reaction plane. Such dispersion alters the magnitude of the observed average in-plane transverse momentum from its true value in beam energy regions where the flow is nonzero. The dispersion can be used to calculate a correction factor that renormalizes the observed in-plane transverse momentum [12]. When the attractive and repulsive scatterings are balanced the magnitude of the observed average in-plane transverse momentum goes to zero, which makes such a renormalization unnecessary.

Information on the compressibility may be obtained through a comparison of the beam energy at which flow disappears to model predictions of that energy. Previous work [8, 13] on the flow excitation function for the ^{40}Ar+^{51}V reaction has shown that it is possible to determine the beam energy at which the attractive and repulsive scatterings are balanced ($E_{\rm bal}$). One can compare the measured energy to a balance energy calculated using microscopic transport codes which employ the BUU formalism. The EOS is incorporated in the formalism through the treatment of the mean field. Other factors such as the uncertain in-medium N-N scattering cross section (σ_{NN}), Coulomb rescattering of the reaction fragments, and nuclear surface effects make it difficult to extract a unique EOS from a single $E_{\rm bal}$ measurement. One solution to this problem may be to map the flow excitation functions and determine $E_{\rm bal}$ for other mass systems. A number of $E_{\rm bal}$ measurements may provide sufficient simultaneous constraints on the BUU calculations to select a unique EOS.

In this work, we have determined some beam energies at which flow is consistent with zero for the ^{139}La+^{139}La and ^{93}Nb+^{93}Nb systems. In Section II we present the experimental details. Section III contains an analysis of the present ^{139}La+^{139}La and ^{93}Nb+^{93}Nb data along with the results of BUU calculations for these reactions. We also summarize all the present experimental measurements of the disappearance of flow. Section IV contains our conclusions.

II. EXPERIMENT

The experiments were performed at the Lawrence Berkeley Laboratory Streamer Chamber Facility. General information on the operation of the streamer chamber can be found elsewhere [14, 15]. Intermediate energy beams of E/A = 160, 112, and 100 MeV for ^{139}La and E/A = 145 and 97 MeV for ^{93}Nb were supplied by the BEVALAC. These ion beams suffered energy losses due to passage through the following absorbers: a 0.13-mm-thick Mylar beam-line exit and 0.08 mm streamer chamber entrance window, an 80 cm air gap separating the beam-line from the chamber, a pair of beam alignment plastic scintillators of thicknesses 0.22 and 0.15 mm, and 30 cm of atmospheric pressure neon gas before the target. Self-supporting 100 mg/cm^2 ^{139}La and ^{93}Nb targets were held in place inside 0.27-mm-thick polyethylene bags to inhibit sparking upon application of the 400 kV Marx generator pulse. The total energy losses from these sources left beam energies at the centers of the targets of E/A = 130, 70, and 50 MeV for ^{139}La and E/A = 120 and 60 MeV for ^{93}Nb, respectively. These energies are accurate to within ±4 MeV. The chamber was located between the poles of a magnet of 1.32 T field strength to provide for fragment rigidity measurements.

Central collision events were selected by a coincidence of scintillator signals. A strong signal from each of the two upstream beam alignment scintillators together with the absence of a large signal in a third scintillator (veto), located 30 cm downstream from the target, provided the trigger. Typically, the downstream veto scintillator threshold was set to 20% of the beam maximum signal. Upon generation of such a trigger coincidence, the Marx generator was discharged and the resulting streamers along the fragment tracks were imaged via the Michigan State University charge-coupled device (MSU-CCD) camera system [16]. Three separate images of the event, taken from different camera locations, were stored in two-dimensional arrays for subsequent analysis. Digitized camera images were also displayed on-line to aid in the electronic trigger adjustments.

Initial off-line analysis of the CCD images consisted of digital image enhancement to eliminate any background light [16]. This was followed by automated track recognition, matching of tracks in the three camera images and three-dimensional track reconstruction [17]. As detailed in Ref. [17], the average light intensities along the reconstructed tracks and the deduced magnetic rigidities were used to achieve partial mass identification for protons through ^{4}He nuclei. Tritons and ^{3}He were separated by an additional rigidity cut.

III. DATA

A. La+La

The data sets for the ^{139}La+^{139}La reaction consisted of 177 events at E/A = 50 MeV, 946 events at E/A = 70 MeV, and 367 events at E/A = 130 MeV. Multiplicity distributions of the reconstructed fragment tracks are shown in Fig. 1 for the three beam energies. Median reconstructed track multiplicities of 18, 22, and 25 were found for E/A = 50, 70, and 130 MeV, respectively. Due to the event-multiplicity–dependent efficiency variation of the automated analysis techniques [17], the actual median multiplicity for the two higher beam energies should be renormalized upward by (10–15)%. The E/A = 50 MeV median value should not require renormalization because it is below the multiplicity (i.e., 20) for which the automated techniques were able to reconstruct all of the found tracks.

An estimate of the impact parameter range selected by the electronic trigger was obtained by comparing simulations of the reaction to the reconstructed track multiplicity data. Superimposed upon the data in Fig. 1 are the results of simulations of the ^{139}La+^{139}La reaction obtained from the FREESCO [18] explosion-evaporation code. These simulations were passed through a streamer chamber acceptance filter before comparison to the data.

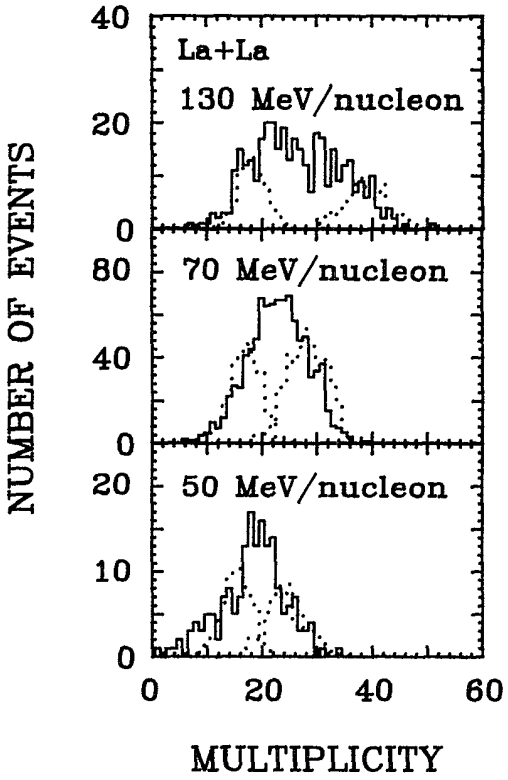

FIG. 1. Multiplicity distributions of reconstructed fragment tracks for the ^{139}La+^{139}La reaction. The solid lines are the measured distributions. Dotted lines are the results of filtered FREESCO simulations as described in the text.

The filter consisted of a low-energy detector threshold of 10 MeV/nucleon, a maximum fragment charge limit of $Z \leq 20$ to accommodate stopping in the target or bag, and a maximum in the number of fragments allowed to hit the veto scintillator. Also, a reduced efficiency for detecting those fragments emitted with laboratory angles directed towards ($\phi = 90° \pm 20°$) and away ($\phi = 270° \pm 45°$) from the CCD cameras was included. This was necessary as such fragments produced very short images on the CCD camera plane. In general, these short tracks are difficult to find and reconstruct by automated techniques [17, 19]. Pions and neutrons were also eliminated by the filter.

The simulations were performed for various fixed fractions of the maximum impact parameter $b_{\max} = R_T + R_P$, where R_T and R_P are the radii of the target and projectile, and $R_{T,P} = 1.17A^{1/3}$. Dotted lines in Fig. 1 indicate two extremes in the impact parameter selection for each beam energy that describe the boundaries of the empirical distribution. At $E/A = 130$ MeV the lower (higher) calculated multiplicity peaks assumed $b = 0.6b_{\max}$ ($0.3b_{\max}$). For $E/A = 70$ MeV and $E/A = 50$ MeV the lower (higher) calculated multiplicity peaks assumed $b = 0.6b_{\max}$ ($0.4b_{\max}$).

Evidence of directed collective motion in the ^{139}La+^{139}La system was obtained by calculating the average in-plane transverse momenta. As defined by Danielewicz and Odyniec [12] the in-plane transverse momentum is

$$p_i^x = \frac{\mathbf{p}_i^\perp \cdot \mathbf{Q}^i}{|\,\mathbf{Q}^i\,|}, \tag{1}$$

in which p_i^x is the transverse momentum in the calculated reaction plane, $\mathbf{p}_i^\perp$ is the component of the momentum vector of fragment i perpendicular to the beam direction, and $\mathbf{Q}^i$ is a vector that characterizes the reaction plane. Conventionally, $\mathbf{Q}^i$ is defined to be

$$\mathbf{Q}^i = \sum_{j \neq i}^{M} \omega_j \mathbf{p}_j^\perp. \tag{2}$$

Here, ω_j is a weighting factor chosen to be $+A_j$ for all fragments emitted in the forward hemisphere of the center-of-mass system and $-A_j$ for those fragments in the backward hemisphere. This weighting factor reflects the larger values of in-plane transverse momentum per nucleon observed for heavier fragments when compared to lighter fragments [20]. Fragment i must be removed from Eq. (2) to avoid self-correlation effects. As detailed in the appendix of Danielewicz *et al.* [21], a correction was applied to the fragments' momentum components to account for the reduced efficiency of finding tracks directed towards and away from the cameras. The leading-order correction for the streamer chamber acceptance consisted of subtracting the average lab transverse momentum at a given rapidity for each fragment type from the transverse momenta that define p_i^x and $\mathbf{Q}^i$. This corrected for the artificial reaction plane generated by the streamer chamber acceptance [21]. The corrected momentum components, designated $p_\nu^{\perp\prime}$, became

$$p_\nu^{\perp\prime}(y) = p_\nu^\perp(y) - < p_\nu^\perp(y) >, \tag{3}$$

where $p_\nu^\perp(y)$ was the νth component of the uncorrected transverse momentum of a particular fragment type and $< p_\nu^\perp(y) >$ was the average over the entire ^{139}La+^{139}La data set of the νth transverse momentum component for that fragment type. The first-order correction defined in Eq. (3) represented a (10-15)% average reduction in the magnitude of $< p^x/A >$ for each rapidity bin.

A multiplicity cut was applied to the data in Fig. 1 in order to predominantly select central collisions. The chosen cuts were event multiplicities greater than 23, 20, and 16 for $E/A = 130$, 70, and 50 MeV, respectively. A three-dimensional fragment-track reconstruction efficiency was then applied to those selected central events. Only those events for which 70% of the fragment tracks in the CCD images were successfully reconstructed in three dimensions were included in subsequent analysis. These cuts reduced the data set sizes to 211 central events at $E/A = 130$ MeV, 670 events at $E/A = 70$ MeV, and 127 events at $E/A = 50$ MeV.

The in-plane transverse momentum spectra [7] for the ^{139}La+^{139}La reaction using the corrected transverse momentum components are presented in Fig. 2. The curves are asymmetric about midrapidity due primarily to the low-energy threshold (near 10 MeV/nucleon) for the streamer chamber. Inefficiency in the automated analysis software also contributed to the asymmetry. The

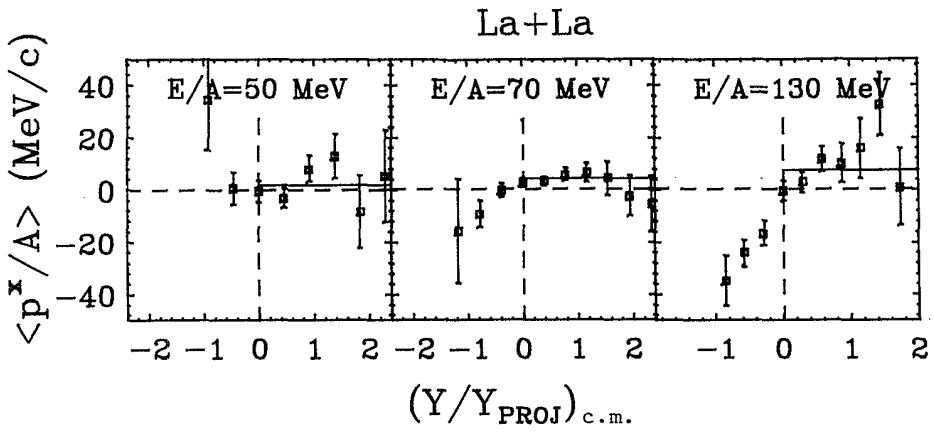

FIG. 2. The in-plane transverse momentum spectra for the ^{139}La+^{139}La reaction. Solid horizontal lines indicate the weighted average flow plateaus.

inefficiency was caused by the presence of very short tracks produced by heavily ionizing fragments. Such short tracks were difficult to distinguish in the region of high track density near the target. In-plane transverse momentum contributions from midrapidity fragments $[(Y/Y_{PROJ})_{rmc.m.} = \pm 0.02]$ were also excluded. This was done because such fragments add little to the reaction plane determination, but contribute to the dispersion of the estimated reaction plane about the true reaction plane [12]. A single quantity to extract from each distribution in Fig. 2 is the flow "plateau" $\overline{< p^x/A >}$ defined as the weighted mean of all $< p^x/A >$ values in the forward center-of-mass hemisphere. The flow plateau eliminates the extra uncertainty from a determination of the slope of the average in-plane transverse momentum at midrapidity, which is used in an alternative definition of flow [25]. We find $\overline{< p^x/A >}$ to be 1.8 ± 3.4, 4.2 ± 2.5, and 7.5 ± 4.5 MeV/c for $E/A = 50$, 70, and 130 MeV data sets, respectively. The quoted errors contain contributions from statistical errors and systematic uncertainties due to fragment misidentification. The latter were estimated by changing the mass identification gates on the track-intensity versus rigidity plots, and recalculating the plateau values for each beam energy. This added a contribution to the errors which was approximately half the magnitude of the statistical uncertainty.

The quoted $\overline{< p^x/A >}$ values have not been renormalized for the dispersion of the estimated reaction plane about the true reaction plane. In principle the dispersion can be estimated by randomly splitting each event into a pair of subevents, then determining the reaction plane using Eqs. (1) and (2) for each subevent. The distribution of the angular difference between the two reaction planes can then be used to estimate a renormalization factor [12]. A reaction plane is manifested by a flat distribution at the larger angles with a peak near zero degrees. In Fig. 3 we present a histogram of the angle differences between the found reaction planes of the subevents for each of the beam energies. A third-order polynomial of minimum χ^2 was fitted to each of the three sets of data points in Fig. 3. The half maximum of the polynomial fit to the $E/A = 130$ MeV data set in Fig. 3 is $(74 \pm 10)°$, which yields an estimated renormalization factor [12] of $1/\cos(37°)$ or 1.25 for the extracted flow at this beam energy. Fitting uncertainties imply that the actual renormalization factor ranges 1.0-2.0. A weaker peak is found in the $E/A = 70$ MeV data with the half

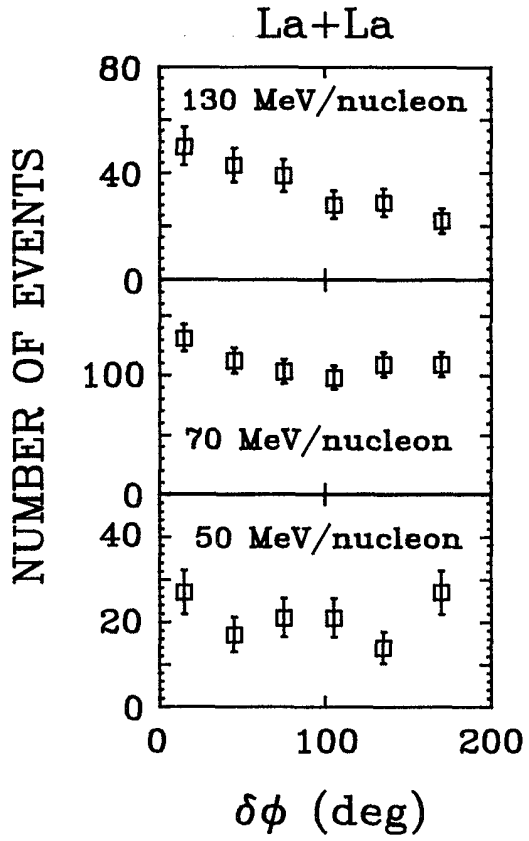

FIG. 3. Angular differences between the reaction planes determined from two randomly created subevents in each full event for ^{139}La+^{139}La.

maximum near 16°, yielding 1.04 as the estimated renormalization factor. Here, the fitting uncertainties give a range 1.0-1.3 for the estimated renormalization factor. It is unclear that such a peak exists in the $E/A = 50$ MeV data. The weak and vanishing peaks in the latter two data sets are expected for beam energy regions of small or disappearing flow, where the reaction plane is not well defined.

A comparison of the ^{139}La+^{139}La data was made to calculations from nuclear transport theory. The BUU equation was solved using a density-dependent one-body potential from Bertsch, Kruse, and Das Gupta [22] augmented by a momentum-dependent potential from Welke *et al.* [23]. As shown by Gale *et al.* [3] this potential, which implies an EOS of $K = 215$ MeV, successfully calculated both the midrapidity slope and plateau values of the observed [21] transverse momentum data for $E/A = 800$ MeV ^{139}La+^{139}La collisions. In Fig. 4, the BUU predictions are compared to the present, renormalized plateau transverse momentum data. The error bars on the empirical data in Fig. 4 represent only statistical uncertainties. The calculations were performed at a fixed impact parameter of $b = 2$ fm, corresponding to an average impact parameter for the innermost (5-6)% of the geometric cross section. A weighting factor of $\Omega = \pm 1$ was selected for fragments emitted in the forward (+1) and backward (−1) center-of-mass direction. This choice is appropriate for these calculations as the BUU is a model for the evolution of the one-body phase space distribution and does not contain contributions from composite fragments. The calculations have also not been modified by the streamer chamber acceptance filter as the filter depends upon knowledge of the fragments' charge. A lack of fragment charge filtering should not be a problem as transverse momentum is generated early in the heavy-ion collision, before the formation of many composite fragments assuming that no rescattering of the fragments takes place. However, the streamer chamber low-energy threshold may reduce the slope of the calculated line. We find that the calculated flow disappears and changes sign in the beam energy region of $E_{\rm bal} \leq 50$ MeV/nucleon for this system. The difference in slope between the BUU predictions and the empirical data may also be attributed to uncertainties in the estimated renormalization factor. In contrast, $E_{\rm bal}$ would not be affected by the uncertainties in the renormalization of the transverse momentum. This insensitivity is due to the fact that at $E_{\rm bal}$ the average directed collective motion has vanished. It would be useful if models that do contain complex fragment production mechanisms, such as the quantum-molecular-dynamics (QMD) [24] model, were used to predict the behavior of the disappearance of flow. Questions of the dependence of $E_{\rm bal}$ on the streamer chamber detector acceptance could then be addressed.

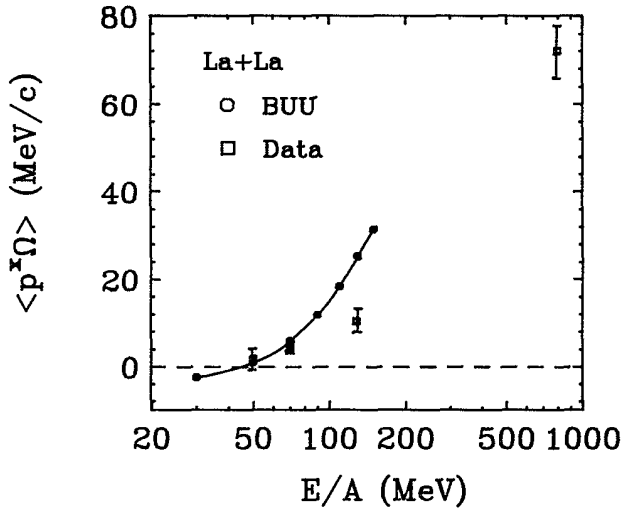

FIG. 4. Comparison of BUU predictions to measurements [7] of the flow excitation function for the ^{139}La+^{139}La reaction. The $E/A = 800$ MeV datum is from [21]. The error bars are statistical and the lines are drawn to guide the eye.

B. Nb+Nb

The data sets for the ^{93}Nb+^{93}Nb reaction contained 379 events at $E/A = 60$ MeV and 262 events at $E/A = 120$ MeV selected via the scintillator coincidence trigger. In Fig. 5 the ^{93}Nb+^{93}Nb reconstructed track multiplicities are presented. Median multiplicities of 16 and 20

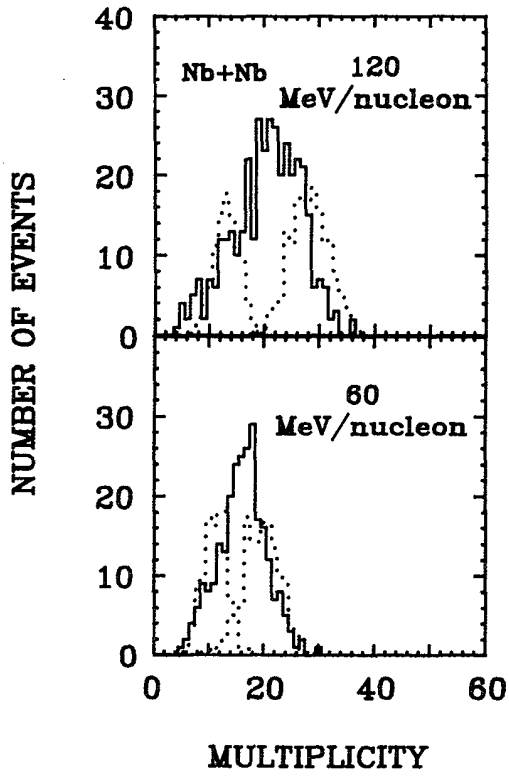

FIG. 5. Multiplicity distributions of reconstructed fragment tracks for the ^{93}Nb+^{93}Nb reaction. Solid lines are the measured distributions and the dotted lines are the results of filtered FREESCO simulations.

were found for the lower and higher beam energies, respectively. These multiplicities should not require upward renormalization as they are in the range for which all of the found tracks were reconstructed by the automated analysis techniques.

In the same manner discussed in Sec. III A, we have estimated the impact parameter range sampled for the ^{93}Nb+^{93}Nb data sets. Superimposed upon the data in Fig. 5 are the results of the FREESCO simulations following passage through the streamer chamber acceptance filter. The deduced impact parameter range is comparable to that obtained for the ^{139}La+^{139}La data sets. For E/A = 120 MeV and E/A = 60 MeV the lower (higher) calculated multiplicity peaks assumed $b = 0.6b_{\max}$ $(0.4b_{\max})$.

A multiplicity cut was applied to the data in Fig. 5 in order to select the central collisions. The chosen cuts were event multiplicities greater than 15 and 12 for E/A = 120 and 60 MeV, respectively. Following the three-dimensional reconstruction efficiency cut, the data set sizes were reduced to 205 events at $E/A = 120$ MeV and 254 events at $E/A = 60$ MeV.

The in-plane transverse momenta spectra, corrected for the streamer chamber acceptance as described by Eq. (3), are shown in Fig. 6. Solid horizontal lines in Fig. 6 denote the flow plateaus extracted from the forward hemisphere $< p^x/A >$ values. The values of $< p^x/A >$ deduced from the data are 4.6 ± 6.3 MeV/c at $E/A = 60$ MeV and 12.0 ± 6.3 MeV/c at $E/A = 120$ MeV. The quoted errors contain statistical and systematic uncertainties as described above. No correction has been applied for the dispersion of the found reaction plane about the true reaction plane. The observed decrease of $< p^x/A >$ as the beam energy drops is in qualitative agreement with the exploratory calculations of Molitoris *et al.* [9]. These authors employed the BUU formalism without a momentum-dependent interaction and used a stiff EOS ($K = 375$ MeV). They predicted that the slope of the in-plane transverse momentum spectra for midrapidity particles from the ^{93}Nb+^{93}Nb reaction should reverse its sign, indicating a change in sign of the scattering angle near $E/A = 50$ MeV beam energy. Equivalently, the predicted flow plateau value would approach zero as observed in the present data.

The flow excitation function has been mapped previously at higher beam energies for the ^{93}Nb+^{93}Nb reaction [25]. A comparison of the present intermediate-energy-flow results to the existing-flow excitation function was made by extracting the slope of the data in Fig. 6 at midrapidity. This was accomplished by following the prescription for the analysis of transverse momentum spectra outlined by the plastic ball group [26]. The dotted lines in this figure represent minimum χ^2 fits using a third-order polynomial. Flow was taken as the coefficient of the first-order term. Uncertainty in the fitting procedure was estimated by varying the data points within their error bars and refitting the third-order polynomial. A correction for the found reaction plane dispersion about the true reaction plane was estimated by the technique described above. In Fig. 7 we show plots of the angular difference between the found reaction planes in the subevents. A third-order polynomial of minimum χ^2 was fitted to the two data sets presented in Fig. 7. An enhancement at $\delta\phi = 0°$ for the $E/A = 120$ MeV data set demonstrates the existence of the reaction plane. The half-maximum of the polynomial fit to the E/A = 120 MeV data set in Fig. 7 is at approximately 66°, which yields a renormalization factor [12] of $1/\cos(33°)$ or 1.2 for the extracted flow at this beam energy. Fitting uncertainties suggest that 1.1-1.4 is the estimated renormalization factor range. For the $E/A = 60$ MeV data in Fig. 7, the values are approximately 74° for the half-maximum, a renormalization factor of 1.3, with a renormalization range 1.1-2.1.

The resulting flow values for the intermediate energy ^{93}Nb+^{93}Nb reaction, renormalized for the reaction plane dispersion, are shown in Fig. 8 along with the existing higher energy portion of the flow excitation function. The error bars on the streamer chamber flow points contain statistical uncertainties, but are dominated by fitting uncertainties from the Fig. 6 data. Obviously, more data points are needed in the beam energy region between 30 and 100 MeV/nucleon before $E_{\rm bal}$ can be accurately measured for the ^{93}Nb+^{93}Nb system.

We have performed some exploratory BUU calculations for the ^{93}Nb+^{93}Nb system for fixed σ_{NN} to examine

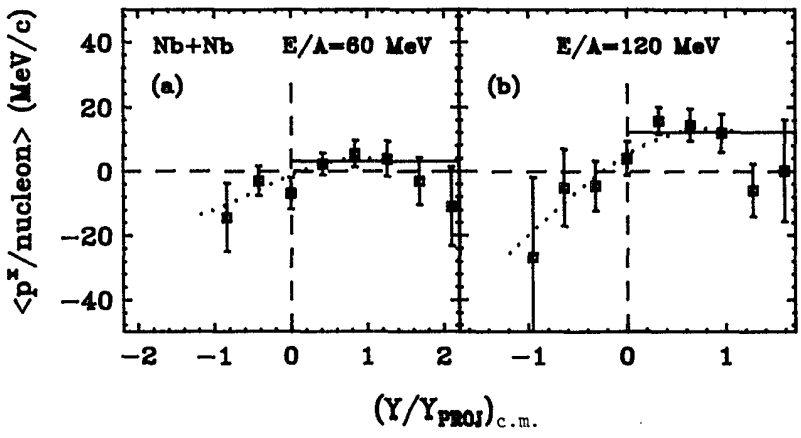

FIG. 6. The in-plane transverse momentum spectra for the ^{93}Nb+^{93}Nb reaction. Solid horizontal lines indicate the weighted average flow plateaus. Dotted lines represent the midrapidity portions of minimum χ^2 fits using a third-order polynomial in the forward and backward center-of-mass rapidity data. The slope of the dotted lines at $(Y/Y_{\rm PROJ})_{\rm c.m.} = 0$ is an alternative definition of flow.

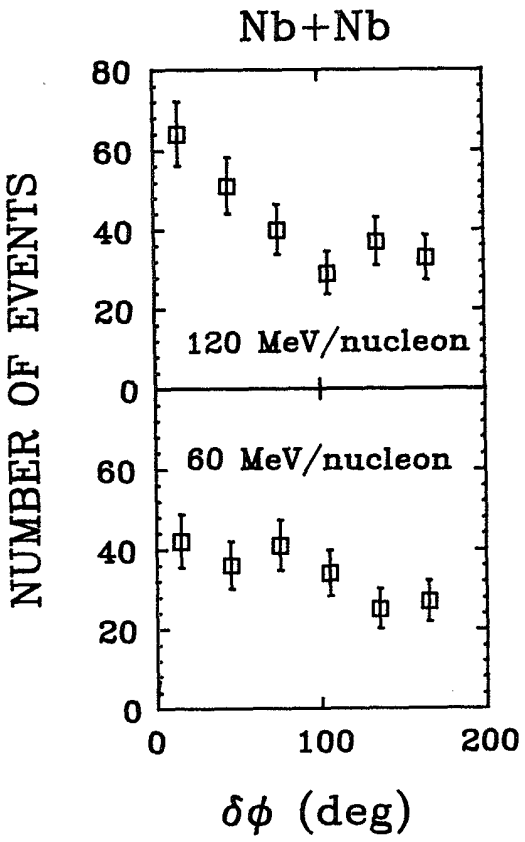

FIG. 7. Angular difference between the reaction planes determined from two randomly created subevents in each full event for ^{93}Nb+^{93}Nb.

the relationship between $E_{\rm bal}$ and the equation of state. Soft ($K = 200$ MeV) and hard ($K = 380$ MeV) equations of state were selected by using different parametrizations of the density-dependent mean-field. Details of the parametrizations may be found elsewhere [2]. The calculations were performed for various beam energies and for the deduced impact parameter ranges taken from the present data. We calculate the quantity $d < p^x/p^\perp > /dy$ which is known as the reduced flow. Here, $p^\perp$ is the total perpendicular momentum of a fragment and p^x is the in-plane component of that momentum. The present exploratory calculations did not include the effects of a momentum-dependent potential. It is already known [11] that the magnitude of the in-plane transverse momentum is sensitive to σ_{NN}. Likewise, Ogilvie *et al.* [8] have shown that for the ^{40}Ar+^{51}V system $E_{\rm bal}$ is dependent upon σ_{NN} as well as the equation of state. We find that for a heavier system and $\sigma_{NN} = \sigma_F$, where σ_F is the free nucleon-nucleon scattering cross-section, a mild sensitivity of $E_{\rm bal}$ to the assumed EOS is maintained. Least-squares fits of straight lines through the calculated data points were used to extract the predicted $E_{\rm bal}$ values. As illustrated in Fig. 9, the calculated $E_{\rm bal}$ changes from 76 ± 4 to 81 ± 4 MeV/nucleon when the assumed EOS is changed from soft to hard. Sensitivity of $E_{\rm bal}$ for the Nb+Nb system to the scattering cross section was also investigated. The calculated reduced-flow curves using

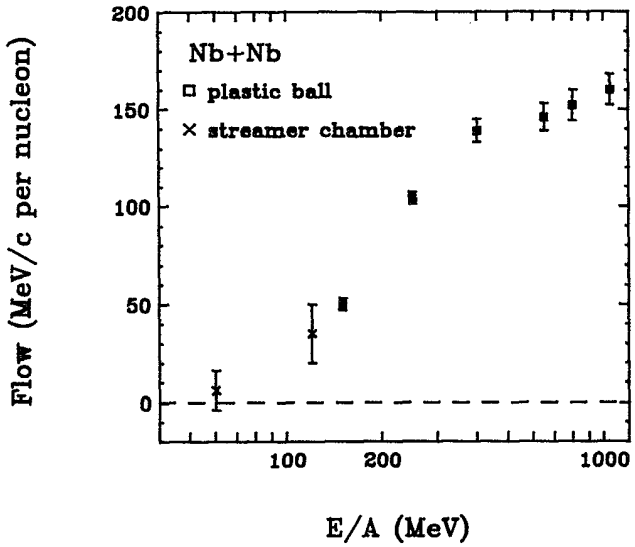

FIG. 8. Flow excitation function for the ^{93}Nb+^{93}Nb reaction. The plastic ball data is taken from Doss *et al.* [25].

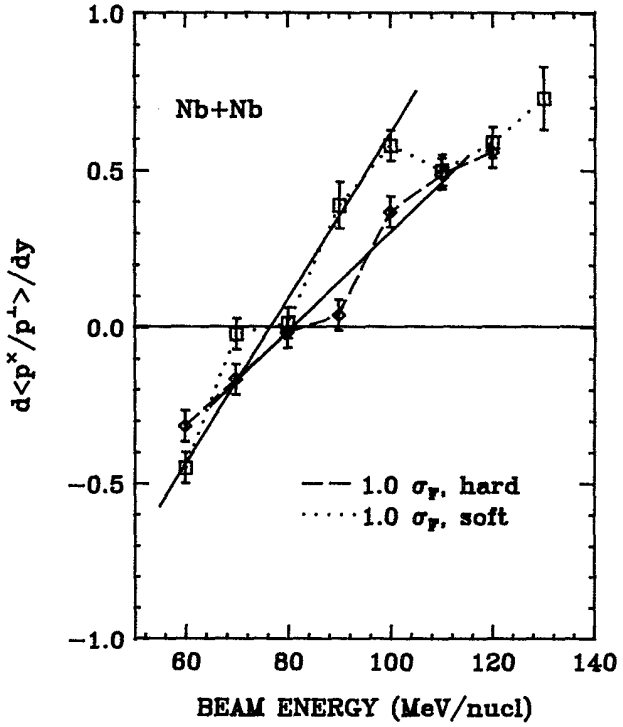

FIG. 9. BUU predictions for $\sigma_{NN} = 1.0\sigma_F$ employing a hard (long dashed line) and soft (dotted line) EOS. Assuming a hard (soft) EOS for the ^{93}Nb+^{93}Nb reaction, a linear fit of the calculated data points in the region of vanishing flow yields a balance energy near $E/A = 81$ (76) MeV. In Ref. [8] similar calculations for a hard (soft) EOS in the ^{40}Ar+^{51}V system resulted in a balance energy of $E/A = 88(80)$ MeV. The solid lines are the results of least-squares fits of straight lines to the data points. All other lines are drawn to guide the eye.

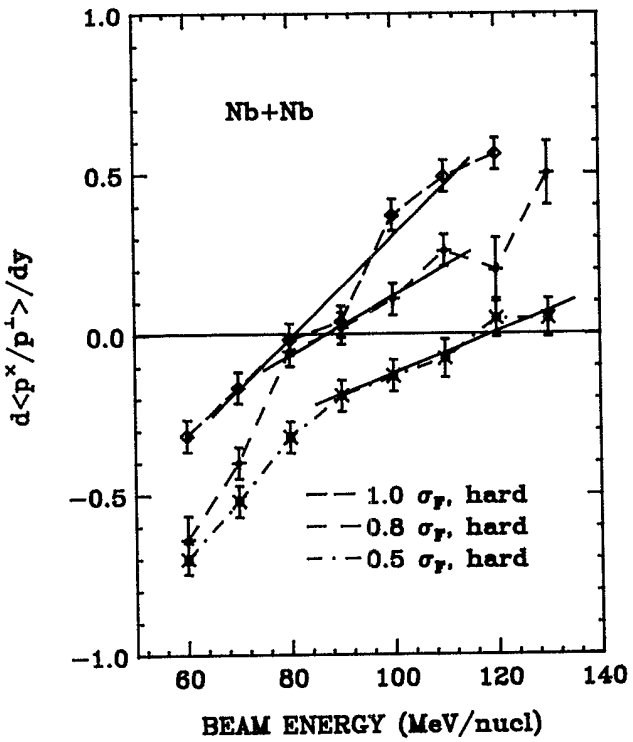

FIG. 10. BUU predictions for several values of σ_{NN} assuming a hard EOS. The solid lines are the results of least-squares fits of straight lines to the data points. All other lines are drawn to guide the eye.

$\sigma_{NN} = 1.0\sigma_F$, $0.8\sigma_F$, and $0.5\sigma_F$ employing a hard EOS are shown in Fig. 10. Least-squares fits of straight lines through the data points yielded $E_{\rm bal} = 81 \pm 4$, 87 ± 4, and 119 ± 4 MeV/nucleon for the three scattering cross-section values. The quoted errors are from fitting uncertainties. Within the constraints of our BUU calculations (no complex fragment formation, no Coulomb scattering or surface effects) our present balance energy for Nb+Nb tends to favor a hard EOS with in-medium scattering cross sections close to the free scattering values.

In Ref. [7] it was also shown that, in the full BUU calculations, the compression built up from the collision term was responsible for the transition from an attractive- to repulsive-dominated reaction mechanism. Here we turn off the collision term by setting σ_{NN} to zero, and examine the purely attractive component of the reaction mechanism. Results of the present calculations suggest that the reduced flow predicted for purely attractive scattering in the ^{93}Nb+^{93}Nb system, illustrated in Fig. 11, is not sensitive to our EOS choice. A comparison to the attractive scattering from the ^{40}Ar+^{51}V system [8] (dotted line in Fig. 11) shows virtually no difference from the Nb+Nb cases.

In Table I we summarize the results on measurements of the disappearance of flow. As suggested by the results of the present BUU calculations, hints of a mass dependence exist in the empirical data. Heavier systems appear to exhibit the disappearance of flow at lower beam energies. The larger number of nucleons in such systems may facilitate the buildup of repulsive pressure from compressed nuclear matter in the interaction zone. Lower beam energies would then be adequate to reach a matter density which generates sufficient repulsive scattering to balance the attractive mean-field strength. The results [29] for the ^{197}Au+^{197}Au system were based upon an extrapolation of the flow data to a potential region of zero flow. It is possible that for such high Z systems, the extra Coulomb repulsion may preclude a measurement of the actual disappearance of flow. It is clear that both the disappearance and reappearance [13] of flow must be observed for each mass system before $E_{\rm bal}$ can be accurately defined.

TABLE I. Empirical mass systematics for the balance energy.

System	$E_{\rm bal}$ (MeV/nucleon)	Reference
Ar+V	85±10	[13]
Ar+Al	70-80	[28]
Nb+Nb	≈ 60	present
La+La	≈ 50	[7]
Au+Au	≤ 60	[29]

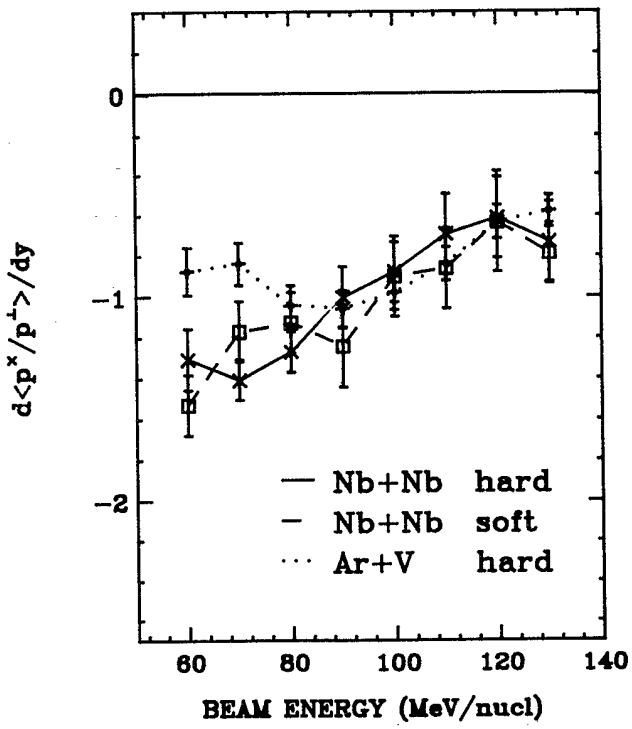

FIG. 11. BUU predictions for the reduced flow due to the purely attractive mean-field interaction ($\sigma_{NN} = 0$). The solid (dashed) lines are the results for the ^{93}Nb+^{93}Nb reaction assuming a hard (soft) EOS. The dotted line indicates the results of a test of the mass dependence in the attractive flow, assuming a hard EOS for the ^{40}Ar+^{51}V reaction. All lines are drawn through the data points to guide the eye.

IV. CONCLUSIONS

In this work, we have mapped portions of the in-plane transverse momentum (known colloquially as flow) excitation functions for the ^{139}La+^{139}La and ^{93}Nb+^{93}Nb reactions at intermediate bombarding energies. It was observed that the flow vanished in the ^{139}La+^{139}La system for a beam energy near 50 MeV/nucleon. Flow was consistent with zero near a beam energy of 60 MeV/nucleon in the lighter ^{93}Nb+^{93}Nb system. The concept of a balance energy [8], defined as that beam energy at which attractive and repulsive scattering strengths are equivalent, was used to interpret the disappearance of flow. Together with the results from studies [7, 8, 28, 29] of the ^{40}Ar+^{51}V, ^{40}Ar+^{27}Al and ^{197}Au+^{197}Au systems, hints of a mass dependence in the disappearance of flow are indicated. Full calculations of the balance energy for ^{93}Nb+^{93}Nb using the BUU model imply that the balance energy is mildly sensitive to the assumed equation of state. It was also deduced that, for a fixed scattering cross section, repulsive scattering at these energies is more sensitive to the assumed EOS than is mean-field attractive scattering.

It would be useful to further study this possible mass dependence of $E_{\rm bal}$ because detailed systematics may help to specify the equation-of-state. Other variables, such as the rapidity distributions of intermediate mass fragments [27] may lead to information on the in-medium scattering cross section which is known to affect the balance energy. Theoretical work on the inclusion of Coulomb repulsion or additional attractive scattering sources is also warranted. Calculations involving different model assumptions, such as those in the quantum-molecular-dynamics [24] approach to heavy-ion collisions, may also aid our understanding of the disappearance of flow.

The work was supported by National Science Foundation under Grant No. PHY-89-13815.

[1] G.E. Brown, Nucl. Phys. **A488**, 689c (1988).
[2] G.F. Bertsch and S. Das Gupta, Phys. Rep. **160**, 189 (1988).
[3] C. Gale, G.M. Welke, M. Prakash, S.J. Lee, and S. Das Gupta, Phys. Rev. C **41**, 1545 (1990).
[4] M.M. Sharma, W.T.A. Borghols, S. Brandenburg, S. Crona, A. van der Woude, and M.N. Harakeh, Phys. Rev. C **38**, 2562 (1988).
[5] Norman Glendenning, Phys. Rev. C **37**, 2733 (1988).
[6] H. Kruse, B.V. Jacak, and H. Stöcker, Phys. Rev. Lett. **4**, 289 (1985).
[7] D. Krofcheck, W. Bauer, G.M. Crawley, C. Djalali, S. Howden, C.A. Ogilvie, A. Vander Molen, R.S. Tickle, G.D. Westfall, W.K. Wilson, and C. Gale, Phys. Rev. Lett. **63**, 2028 (1989).
[8] C.A. Ogilvie, W. Bauer, D.A. Cebra, J. Clayton, S. Howden, J. Karn, A. Nadasen, A. Vander Molen, G.D. Westfall, W.K. Wilson, and J.S. Winfield, Phys. Rev. C **42**, R10 (1990).
[9] J. Molitoris, D. Hahn, and H. Stöcker, Nucl. Phys. **A447**, 13c (1986).
[10] M.B. Tsang, R.M. Ronningen, G. Bertsch, Z. Chen, C.B. Chitwood, D.J. Fields, C.K. Gelbke, W.G. Lynch, T. Nayak, J. Pochodzalla, T. Shea, and W. Trautmann, Phys. Rev. Lett. **57**, 559 (1986).
[11] G.F. Bertsch, W.G. Lynch and M.B. Tsang, Phys. Lett. **189B**, 384 (1987).
[12] P. Danielewicz and G. Odyniec, Phys. Lett. **157B**, 146 (1985).
[13] D. Krofcheck, D.A. Cebra, M. Cronqvist, R. Lacey, T. Li, C.A. Ogilvie, A. Vander Molen, K. Tyson, G.D. Westfall, W.K. Wilson, J.S. Winfield, A. Nadasen, and E. Norbeck, Phys. Rev. C **43**, 350 (1991).
[14] K. van Bibber and A. Sandoval, *Heavy Ion Science*, edited by D. Bromley (Plenum, New York, 1985).
[15] A. Sandoval, R. Bock, R. Brockmann, A. Dacal, J.W. Harris, M. Maier, M.E. Ortiz, H.G. Pugh, W. Rauch, R.E. Renfordt, F. Reiss, L.S. Schroeder, R. Stock, H. Ströbele, and K.L. Wolf, Nucl. Phys. **A400**, 365c (1983).
[16] S.A. Angius, R. Au, G.M. Crawley, C. Djalali, R. Fox, M. Maier, C.A. Ogilvie, A. Vander Molen, G.D. Westfall, and R.S. Tickle, Nucl. Instrum. Methods **A273**, 283 (1988).
[17] D. Krofcheck, G.M. Crawley, C. Djalali, S. Howden, C.A. Ogilvie, A. Vander Molen, G.D. Westfall, W.K. Wilson, and R.S. Tickle, Nucl. Inst. Meth **A288**, 497 (1990).
[18] G. Fai and J. Randrup, Comput. Phys. Commun. **42**, 385 (1986).
[19] H. Ströbele, Nucl. Instrum. Methods **A221**, 523 (1984).
[20] K. Doss, H.Å. Gustafsson, H. Gutbrod, J. Harris, B. Jacak, K. Kampert, B. Kolb, A. Poskanzer, H. Ritter, H. Schmidt, L. Teitelbaum, M. Tincknell, S. Weiss, and H. Weiman, Phys. Rev. Lett. **59**, 2720 (1987).
[21] P. Danielewicz, H. Ströbele, G. Odyniec, D. Bangert, R. Bock, R. Brockmann, J.W. Harris, H.C. Pugh, A. Sandoval, L.S. Schroeder, and R. Stock, Phys. Rev. C **38**, 120 (1988).
[22] G.F. Bertsch, H. Kruse, and S. Das Gupta, Phys. Rev. C **29**, 673 (1984).
[23] G. Welke, M. Prakash, T.T.S. Kuo, S. Das Gupta, and C. Gale, Phys. Rev. C **38**, 2101 (1988).
[24] J. Aichelin and H. Stöcker, Phys. Lett. B **176**, 14 (1986).
[25] K.G.R. Doss, H.Å. Gustafsson, H.H. Gutbrod, K.H. Kampert, B. Kolb, H. Löhner, B. Ludewigt, A.M. Poskanzer, H.G. Ritter, H.R. Schmidt, and H. Wieman, Phys. Rev. Lett. **57**, 302 (1986).
[26] H.H. Gutbrod, A.M. Poskanzer, and H.G. Ritter, Rep. Prog. Phys. **52**, 1267 (1989).
[27] G. Peilert, H. Stöcker, W. Greiner, A. Rosenhauer, A. Bohnet, and J. Aichelin, Phys. Rev. C **39**, 1402 (1989).
[28] J.P. Sullivan, J. Péter, D. Cussol, G. Bizard, R. Brou, M. Louvel, J.P. Parry, R. Regimbart, J.C. Steckmeyer, B. Tamain, E. Crema, H. Doubre, K. Hagel, G.M. Jin, A. Peghaire, F. Saint-Laurent, Y. Cassagnou, R. Legrain, C. Lebrun, E. Rosato, R. McGrath, S.C. Jeong, S.M. Lee, Y. Nagashima, T. Nakagawa, M. Ogihara, J. Kasagi, and T. Motobayashi, Phys. Lett. B **249**, 8 (1990).
[29] W.M. Zhang, R. Madey, M. Elaasar, J. Schambach, D. Keane, B.D. Anderson, A.R. Baldwin, J. Cogar, J.W. Watson, G.D. Westfall, G. Krebs, and H. Wieman, Phys. Rev. C **42**, R491 (1990).